

# SHORTER COMMUNICATIONS

## TRANSIENT TEMPERATURE RESPONSE OF CHARRING COMPOSITE SLABS

JOHN E. PRUSSING and HERMAN KRIER

Department of Aeronautical and Astronautical Engineering, University of Illinois at Urbana—Champaign, Urbana, IL 61801, U.S.A.

(Received 9 August 1976 and in revised form 28 June 1977)

### NOMENCLATURE

$A$ ,	tridiagonal matrix of nondimensional coefficients;
$b_j$ ,	value of $\xi$ at boundary of $j$ th layer;
$\bar{H}$ ,	latent heat of wood [J/kg];
$h$ ,	mesh point separation [m];
$k$ ,	thermal conductivity [W/m K];
$L$ ,	total length of slab [m];
$m$ ,	number of layers in slab;
$n$ ,	number of mesh points;
$q$ ,	heat flux [W/m <sup>2</sup> ];
$T_c$ ,	critical temperature [K];
$T_0$ ,	initial temperature [K];
$t$ ,	time [s];
$u$ ,	nondimensional vector of forcing terms;
$x$ ,	distance coordinate through slab [m];
$Z$ ,	heat loss term due to charring [W/m K].

### Greek symbols

$\alpha$ ,	thermal diffusivity [m <sup>2</sup> /s];
$\alpha^*$ ,	nondimensionalized diffusivity;
$\theta$ ,	nondimensional temperature difference;
$\xi$ ,	nondimensional distance coordinate through slab;
$\rho$ ,	density [kg/m <sup>3</sup> ];
$\tau$ ,	nondimensional time ( $\approx$ Fourier number).

### Subscripts

$ch$ ,	conditions in the charred layer;
$fo$ ,	fall-off condition;
$i$ ,	at the $i$ th mesh point ( $i = 1, 2, \dots, n$ );
$j$ ,	in the $j$ th layer ( $j = 1, 2, \dots, m$ );
$l_j$ ,	value of $i$ at boundary of $j$ th layer;
$w$ ,	conditions in wood layer.

### INTRODUCTION

PREDICTION of the unsteady temperature distribution in composite slabs by solving the one-dimensional heat equation has been studied by many investigators [1-6]. These studies differ in the heat flux boundary conditions, the boundary conditions between domains, and the methods of integration of the differential equations. An analysis of some numerical methods for heat transfer was also made by Segletes [7].

In this investigation a simplified model is constructed to predict the transient temperature response in a finite composite slab in which one or more of the layers may char or decompose at high temperature. The complexity introduced by this phenomenon is that an additional layer (of char) appears after some critical temperature has been reached, and the thickness of this layer varies with time at a rate which depends on the local time-dependent temperature distribution.

The temperature response of single-slab, charring ablators and other decomposing materials has been studied [8, 9]. However, solutions to the composite slab problem with

charring material are more difficult. In addition, if the thermal properties of the layers are very different, the system of differential equations to be numerically integrated becomes numerically "stiff".

A complete analysis of the temperature response of charring materials would require the solution of additional equations of degasification continuity and pyrolysis reactions [8]. In this investigation the model instead assumes that the char begins to form at some critical temperature and later begins to fall off as a higher critical temperature is reached. This region of charred material then has a thickness which varies with time and a thermal diffusivity which is different from that of the virgin slab.

Solutions presented here, except for one comparison example, assume a known, constant heat flux at one face of the composite slab. After charring occurs, an additional layer of char appears between the applied heat and the original uncharred slab. By symmetry arguments the boundary condition at the cold face of the composite slab is a zero temperature gradient.

The numerical integration scheme used to solve the stiff system of differential equations for the composite slab has been tested against a known composite slab solution without char [5]. The results compare very favorably with previously obtained solutions.

### ANALYSIS

#### Single slab

The model for the composite slab problem is based on the one-dimensional heat equation for a single material of finite thickness  $L$ :

$$\frac{\partial T(x, t)}{\partial t} = \alpha \frac{\partial^2 T(x, t)}{\partial x^2}, \quad t \geq 0, \quad 0 \leq x \leq L \quad (1)$$

where  $T(x, t)$  is the temperature and  $\alpha$  is the thermal diffusivity of the material, assumed to be independent of temperature. For a symmetrically heated slab of thickness  $2L$  the initial and boundary conditions are

$$T(x, 0) = T_0 \quad (2)$$

$$q(L, t) = -k \frac{\partial T(L, t)}{\partial x} \quad (3)$$

$q(L, t)$  is the specified heat flux, and  $k$  is the thermal conductivity of the material. Due to the definition of  $x$  the specified heat flux is negative. Also by symmetry

$$q(0, t) = -k \frac{\partial T(0, t)}{\partial x} = 0. \quad (4)$$

One can conveniently nondimensionalize the problem by defining a nondimensional distance  $\xi \triangleq x/L$ , a nondimensional time  $\tau \triangleq t\alpha/L^2$  and a nondimensional temperature difference:

$$\theta(\xi, \tau) \triangleq \frac{T(\xi, \tau) - T_0}{T_c - T_0}, \quad (5)$$

where  $T_0$  is the initial temperature [equation (2)] and  $T_E$  is a higher, critical temperature for one of the layers such as a charring temperature or an ignition temperature of a combustible solid. In terms of these nondimensional variables, the interval  $t \geq 0$  remains as  $\tau \geq 0$ ,  $0 \leq x \leq L$  becomes  $0 \leq \xi \leq 1$ , and  $T_0 \leq T \leq T_E$  becomes  $0 \leq \theta \leq 1$ . The heat equation (1) is then

$$\frac{\partial \theta(\xi, \tau)}{\partial \tau} = \frac{\partial^2 \theta(\xi, \tau)}{\partial \xi^2} \quad (6)$$

and the initial and boundary conditions (2–4) become

$$\theta(\xi, 0) = 0 \quad (7)$$

$$\frac{\partial \theta(1, \tau)}{\partial \xi} = \frac{-q(1, \tau)L}{k(T_E - T_0)}, \quad (8)$$

where  $q(1, \tau)$  is the specified heat flux and, at the cold end:

$$\frac{\partial \theta(0, \tau)}{\partial \xi} = 0. \quad (9)$$

#### Composite slabs

Consider a composite slab composed of  $m$  individual layers. The  $j$ th layer for  $j = 1, 2, \dots, m$  occupies the domain  $b_j \leq \xi < b_{j+1}$ , with  $b_1 = 0$  and  $b_{m+1} = 1$ . In general each of the layers will have different thermal properties. Distance and temperature in the composite slab can be nondimensionalized as described above in terms of  $\xi$  and  $\theta$ . However, time can be nondimensionalized only in terms of one of the diffusivities of the materials. If  $\alpha_j$  is the diffusivity in the  $j$ th layer, one can define  $\tau = t\alpha_j/L^2$ , and the heat equation (6) becomes, in the  $j$ th layer:

$$\frac{\partial \theta(\xi, \tau)}{\partial \tau} = \alpha_j^* \frac{\partial^2 \theta(\xi, \tau)}{\partial \xi^2}, \quad (10)$$

where  $\alpha_j^* \triangleq \alpha_j/\alpha_1$  for  $j = 1, 2, \dots, m$ .

The initial condition for the temperature in the composite slab is given by equation (7), and the boundary condition at the cold end of the slab is given by equation (9). The boundary condition at the hot end is, in terms of the specified heat flux  $q(1, \tau)$ :

$$\frac{\partial \theta(1, \tau)}{\partial \xi} = \frac{-q(1, \tau)L}{k_m(T_E - T_0)}, \quad (11)$$

where  $k_m$  is the conductivity of the  $m$ th layer. In addition to these boundary conditions, there exist continuity conditions at the boundary  $b_j$  between layers for  $j = 2, 3, \dots, m$  of the form

$$\theta(b_j^-, \tau) = \theta(b_j^+, \tau), \quad (12)$$

where  $b_j^-$  is a value of  $\xi$  slightly smaller than  $b_j$  and  $b_j^+$  is a value slightly larger. Another continuity condition (the energy balance) is:

$$k_{j-1} \frac{\partial \theta(b_j^-, \tau)}{\partial \xi} = k_j \frac{\partial \theta(b_j^+, \tau)}{\partial \xi}. \quad (13)$$

Equation (12) represents the fact that the temperature is continuous across a boundary between layers, while the equation (13) implies that the heat flux is continuous, although, because of the different conductivities the temperature gradient is discontinuous. One instance where equation (13) will be modified is for the charring of wood. In this case a heat loss occurs at the char-wood boundary which is proportional to the product of the latent heat of wood and the charring rate.

#### Finite difference analysis

To solve the heat equation (10) with initial condition (7) and boundary conditions (9) and (11)–(13), the distance variable  $\xi$  is discretized using finite difference techniques. A set of ordinary differential equations results which can be numerically integrated over the independent variable  $\tau$ . Some composite slab problems can be solved analytically [6], but in

the case of a moving char boundary, a numerical solution must be used.

The interval  $0 \leq \xi \leq 1$  can be discretized into  $n-1$  sub-intervals of length  $h = 1/(n-1)$  by letting  $\xi_i = (i-1)h$  be the mesh point locations,  $i = 1, 2, \dots, n$ . In [11] a derivation of the finite difference equations (14)–(18) below is given. In terms of  $\theta_i(\tau) \triangleq \theta(\xi_i, \tau)$  and

$$\dot{\theta}_i \triangleq \frac{d\theta_i}{d\tau} = \frac{\partial \theta(\xi_i, \tau)}{\partial \tau}, \quad (14)$$

the heat equation (10) and associated boundary conditions are given by

$$\dot{\theta}_i = \alpha_j^* (\theta_{i+1} - 2\theta_i + \theta_{i-1})/h^2 \quad (15)$$

for all  $i \neq l_j$ ,  $j = 1, 2, \dots, m$ , where the  $l_j$  are the ends ( $l_1 = 1$ ,  $l_{m+1} = n$ ) and the boundaries between layers ( $j = 2, \dots, m$ ) [ $b_j = (l_j - 1)h$ ]. The differential equation for mesh point  $l_1 = 1$  (the cold end) is

$$\dot{\theta}_1 = 2\alpha_1^* (\theta_2 - \theta_1)/h^2. \quad (16)$$

For mesh point  $l_{m+1} = n$  (the hot end) it is

$$\dot{\theta}_n = 2\alpha_m^* \left[ \theta_{n-1} - \theta_n + \left( \frac{\partial \theta}{\partial \xi} \right)_n h \right] / h^2 \quad (17)$$

For the other  $l_j$ ,  $j = 2, 3, \dots, m$  the equations which incorporate the continuity conditions are

$$\dot{\theta}_{l_j} = 2 \left( \frac{\alpha_{j-1}^* \alpha_j^*}{h^2} \right) \times \left[ \frac{k_j \theta_{l_j+1} - (k_j + k_{j-1}) \theta_{l_j} + k_{j-1} \theta_{l_j-1}}{k_j \alpha_{j-1}^* + k_{j-1} \alpha_j^*} \right]. \quad (18)$$

The set of differential equations (15)–(18) can be written in matrix form in terms of the vector  $\theta(\tau)$  having elements  $\theta_i(\tau)$ , as

$$\dot{\theta} = A\theta + u; \quad \theta(0) = 0, \quad (19)$$

where  $A$  is a constant (time-varying in the case of a moving boundary)  $n \times n$  tridiagonal matrix. The elements of  $A$  are functions of the mesh size  $h$  and the thermal properties  $\alpha_j^*$  and  $k_j$ . The vector  $u$  has all elements equal to zero except the last ( $i = n$ ) which is equal to  $2\alpha_m^* (\partial \theta / \partial \xi)_n / h$  [equation (17)]. If the layers have appreciably different thermal properties, the system of equation (19) is numerically stiff. For this reason, the numerical integration routine DIFSUB, developed by Gear [10] is used. This integrator is a multi-step, variable step size method suitable for stiff systems. The variable step size capability allows the integrator to select its own time-step size based on a specified error criterion. A more detailed description of the complete computer program developed to handle composite slabs with charring is given in [11].

#### Charring and decomposition

When one of the layer materials can char or otherwise decompose, e.g. wood, the previous results must be modified. When the temperature of the surface of the wood reaches a critical temperature  $T_{ch}$ , assumed to be of the order of 550 K, the wood begins to char. Several changes result: (i) the layer which was originally wood becomes two layers, wood and char, having different thermal properties, (ii) there is a heat loss at the wood-char boundary due to the charring process, and (iii) as the surface of the char layer reaches a higher critical temperature  $T_{fo}$ , the char begins to fall off, simulating the formation of a porous ash. This fall-off has the effect of moving the heat source to the current location of the surface of the char layer.

As the temperature of the slab increases and more char is formed, the wood-char boundary moves through the wood. The location of this time-varying boundary is simply the location in the wood where the temperature has reached the value  $T_{ch}$ . Analogously the char fall-off location is the point in the char at which the temperature has reached  $T_{fo} > T_{ch}$ . These locations are monitored as the heat equation is numerically integrated. Adjustments in the thickness of the

char and wood layers are made automatically. As the fall-off location passes each mesh point, the number  $n$  of differential equations to be integrated decreases.

The heat loss at the wood-char boundary can be modeled as

$$-q_{ch} = -q_w + \rho_w H |dx_{ch}/dt|. \quad (20)$$

where the subscripts refer to char and wood.  $-q_w$  is the heat flux into the wood from the hotter char and is less than the heat flux from the char  $-q_{ch}$  due to the heat loss in charring. This loss is given by the product of  $\rho_w$  (density of wood),  $H$  (latent heat of wood) and the magnitude of the charring rate—the time derivative of  $x_{ch}$ , the location of the wood-char boundary. (Due to the definition of  $x$ ,  $x_{ch}$  decreases with time.)

As char begins to form, the number of layers  $m$  in the composite slab increases by one. If the wood was originally layer  $m$  nearest the heat source it now becomes layer  $m-1$  with char being layer  $m$ . Because the wood and char have different thermal conductivities, the thermal gradient  $\partial\theta(1, \tau)/\partial\xi$  [equation (11)] at the surface of the slab must be modified for the same heat flux by scaling it by the ratio  $k_{m-1}/k_m (=k_w/k_{ch})$ . This results in a smaller gradient since the conductivity of char is assumed to be greater than that of wood. However, the flow of heat into the slab is not decreased since the diffusivity of char is typically larger than that of wood due to the low density of char.

A similar modification is automatically made when all of the wood has charred and all of the char is fallen off. At this point in the computation the number of layers  $m$  is decreased by two and the gradient is again rescaled. If the new  $m$ th layer can char, a new charring problem is begun. If it cannot, a simple heat conduction model is integrated.

For the heat flow across the wood-char boundary ( $i = l_m$ ) equation (13) is modified using equation (20) to be

$$k_m \left( \frac{\partial\theta}{\partial\xi} \right)_{l_m} = k_{m-1} \left( \frac{\partial\theta}{\partial\xi} \right)_{l_m} + \frac{\rho_w H x_1 |\dot{\xi}_{ch}|}{T_E - T_0}. \quad (21)$$

Equation (18) then becomes for  $i = l_m$

$$\dot{\theta}_i = 2 \left( \frac{\alpha_m^* \alpha_{m-1}^*}{h^2} \right) \times \left[ \frac{k_m \theta_{i+1} - (k_m + k_{m-1}) \theta_i + k_{m-1} \theta_{i-1} - Z}{k_m \alpha_{m-1}^* + k_{m-1} \alpha_m^*} \right]. \quad (22)$$

where

$$Z \triangleq \frac{h \rho_w H \alpha_1 |\dot{\xi}_{ch}|}{T_E - T_0} \quad (23)$$

represents the heat loss due to charring.

In matrix form [equation (19)] the factor  $Z$  introduces an additional non-zero component into the  $n$ -dimensional vector  $\mathbf{u}$ . The  $l_m$ th component of  $\mathbf{u}$  is given by the dimensionless value

$$u_{l_m} = \frac{2 \alpha_m^* \alpha_{m-1}^* \rho_w H \alpha_1 |\dot{\xi}_{ch}|}{(T_E - T_0)(k_m \alpha_{m-1}^* + k_{m-1} \alpha_m^*)}. \quad (24)$$

Note that the value of  $l_m < n$  decreases as the wood-char boundary moves through the wood and the value of  $n$  decreases as the heated char falls off.

The charring rate  $\dot{\xi}_{ch}$  which is required in equations (21) and (24) can be inferred from the rates of change of temperatures at the mesh points on either side of the current wood-char boundary. In terms of the  $l_m$ th mesh point defined such that  $\theta_{l_m} < \theta_{ch}$  and  $\theta_{l_m+1} \geq \theta_{ch}$ , a linear interpolation gives the charring rate as

$$\dot{\xi}_{ch} = -h \left[ \frac{(\theta_{l_m+1}(\theta_{ch} - \theta_{l_m}) + \theta_{l_m} \theta_{l_m+1} - \theta_{ch})}{(\theta_{l_m+1} - \theta_{l_m})^2} \right]. \quad (25)$$

In this expression the temperature rates  $\dot{\theta}_{l_m}$  and  $\dot{\theta}_{l_m+1}$  are known from the differential equations (22) and (15).  $\dot{\xi}_{ch}$  is negative due to the definition of  $\xi$ .

Note that equation (25) causes equation (19) to become nonlinear.

## RESULTS

In Fig. 1 the temperature profiles at three different times are shown for a composite slab. The slab is composed of layers of wood, steel, gypsum and explosive to simulate packaging of an explosive. In this simulation  $T_E$  of equation (5) was taken to be the ignition temperature of the explosive 450 K; thus when  $\theta = 1$  at mesh point number 15 in Fig. 1, the explosive is said to ignite. The total number of mesh points is  $n = 51$ , the magnitude of the heat flux is  $0.418 \text{ MW m}^{-2}$  and the total slab length is 2.54 cm.

As shown in Fig. 1, at  $t = 19 \text{ s}$  the wood has charred as far as the 45th mesh point, where  $\theta = 1.6$ . Some time later, at

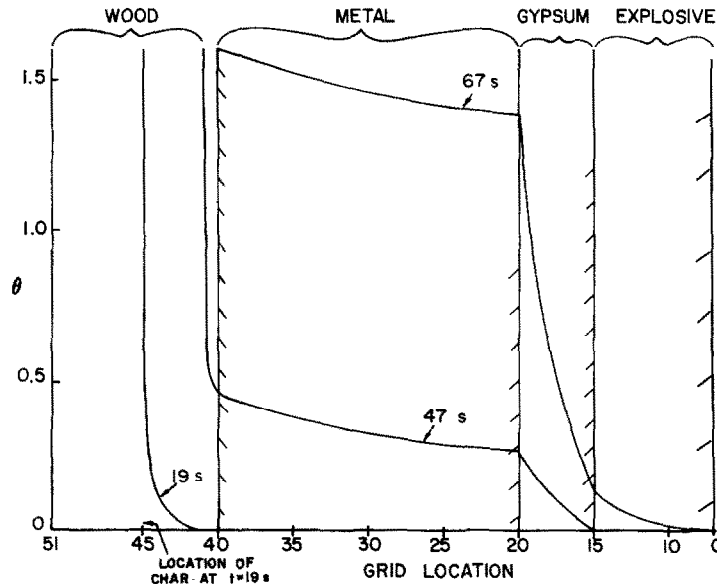


FIG. 1. Temperature profiles in a composite slab.

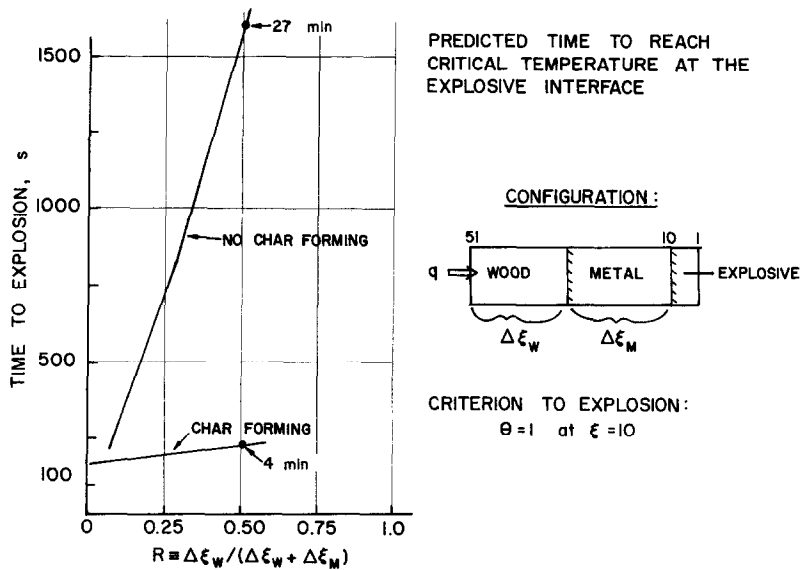


FIG. 2. Predicted time to explosion.

$t = 47$  s, the char boundary is located at mesh point number 41. Due to the high thermal diffusivity of steel, the temperature drop through the steel layer is quite small compared to the other layers. At  $t = 67$  s all of the wood has charred and fallen off and the temperature at the explosive surface (mesh point 15) has reached  $\theta = 0.12$ . At this point the computation continued as a simple heat flow calculation until  $\theta$  at the surface of the explosive reached unity at  $t = 117$  s.

One important application of this study is the ability to predict the time required to reach a critical temperature at one of the interfaces between layers of a composite slab. Calculations were carried out on a three-layered slab composed of wood, metal and explosive. The total length of the slab  $L$  was fixed at 2.54 cm and solutions were obtained for different thickness of wood and metal for a fixed explosive layer thickness. Figure 2 shows the predicted time to explosion as a function of the ratio  $R$  of wood layer thickness to the sum of the thickness of the wood and metal layers. Explosion occurs when  $\theta = 1$  at the metal-explosive interface at mesh point 10.

Two models were considered, one allowing the wood to char and fall off, the other without including char or fall off. One observes in Fig. 2 a dramatic difference obtained by including the realistic condition of char and fall-off. For  $R = 0.5$  (equal thickness of wood and metal) the predicted time to explosion without including char and fall-off is 27 min. Including char and fall-off yields a time to explosion of only 4 min. The imposed heat flux for these calculations was  $0.418 \text{ MW m}^{-2}$ .

The result shown in Fig. 2 is only one example of the use of this simplified model which includes char and fall-off. Many other applications exist, such as optimum packaging of explosives and other hazardous materials, in which a prediction of the time to reach a critical condition is an important design parameter.

## REFERENCES

1. E. Mayer, Heat flow in composite slabs, *ARS JI* **22**, 150-158 (1952).
2. J. J. Brogan and P. J. Schneider, Heat conduction in a series composite wall, *J. Heat Transfer* **83C**, 506-508 (1961).
3. Z. U. A. Warsi and N. K. Choudhury, Weighting function and transient thermal response of buildings—II. Composite structure, *Int. J. Heat Mass Transfer* **7**, 1323-1333 (1964).
4. G. P. Mulholland and M. H. Cobble, Diffusion through composite media, *Int. J. Heat Mass Transfer* **15**, 147-160 (1972).
5. S. Sugiyama, M. Nishimura and H. Watanabe, Transient temperature response of composite slabs, *Int. J. Heat Mass Transfer* **17**, 875-883 (1974).
6. H. Domingos and D. Voelker, Transient temperature rise in layered media, *J. Heat Transfer* **98C**, 329-330 (1976).
7. J. A. Segletes, Explicit numerical method for solution of heat transfer problems, *AIAA JI* **12**, 1463-1464 (1974).
8. R. M. Clever and V. E. Denny, Response of charring ablators to severe aerodynamic and erosion environment, *J. Spacecraft Rockets* **12**, 558-564 (1975).
9. A. M. Kanury, Thermal decomposition kinetics of wood pyrolysis, *Combust. Flame* **18**, 75-83 (1972).
10. C. W. Gear, The automatic integration of ordinary differential equations, *Comm. ACM* **14** (1971). FOR-TUOI Write-up for DIFSUB, Computing Services Offices, University of Illinois at Urbana-Champaign (1975).
11. J. E. Prussing and H. Krier, *Transient Temperature Response of Charring Composite Slabs*, AAE Rep. No. 76-4, Department of Aeronautical and Astronautical Engineering, University of Illinois at Urbana-Champaign (1976).